

Double refracting interferometer with variable direction of tilt laterally sheared wavefronts*

MAKSYMILIAN PLUTA

Central Optical Laboratory, ul. Kamionkowska 18, 03-805 Warszawa, Poland.

A new interferometer for testing microscope objectives has been developed. The interferometer uses polarized light and double refracting elements: Wollaston prisms and a birefringent fibre. The Wollaston prism produces a lateral wavefront shear, whereas the birefringent fibre is used as a secondary light source which together with a rotatable condenser slit diaphragm produces variable directions and amounts of tilt of laterally sheared wavefronts. The interference pattern is observed in the exit pupil of the objective under examination.

1. Introduction

Imagine a diaphragm with a very narrow slit placed in the object plane of an aberration-free microscope objective. The slit is illuminated with a light beam parallel to the objective axis and can be treated as the Dirac delta function $\delta(x)$. Its Fourier transform, $T[\delta(x)]$, arises in the back focal plane of the objective. If u denotes the spatial frequency in the direction x perpendicular to the slit in the object plane, then $T[\delta(x)] = F(u) = 1$. This means that the wavefront is a plane surface in the Fourier plane and has the same amplitude across the whole exit pupil of objective (it has been assumed that the objective does not absorb the light across its exit pupil).

When the objective suffers from aberrations, a deformed in-phase Fourier transform of the δ -function arises. This optical transform may be observed as an interference pattern when the objective is followed by a wavefront shearing interferometer.

2. Preceding interference system

The Fourier transform mentioned above can be observed by means of lateral wavefront shearing interferometer, such as shown in Fig. 1. This interferometer designed many years ago [1, 2] is successfully used for testing microscope objectives in the Central Optical Laboratory, Warsaw, and Polish Optical Works (PZO).

* This work has been presented at the VI Polish-Czechoslovakian Optical Conference, Lubiatów (Poland), September 25-28, 1984.

General working principle of the interferometer is as follows. A divergent light beam, polarized linearly by the polarizer P_1 , leaves the slit S . When passing through the objective Ob the wavefront Σ is subjected to phase retardations corresponding to optical path differences occurring in the optical system of the objective. The image-forming wavefront Σ' is split by the prism W into two wavefronts Σ_1 and Σ_2 (not shown in Fig. 1), polarized at right angles. When passing through the polarizer P_2 , both wavefronts interfere with each other. An interference pattern is observed in the Fourier plane of the objective Ob when a low-power auxiliary microscope M is focussed onto this plane. If the prism W is adjusted so that its centre is brought into coincidence with the slit image S' produced by the aberration-free objective, then a uniform field interference pattern is obtained over the area where the sheared wavefronts Σ_1 and Σ_2 overlap (Fig. 2a). Otherwise, there occur the parallel interference fringes (Fig. 2b). The smaller the interfringe spacing b is, the greater the distance between the slit image S' and the birefringent prism centre.

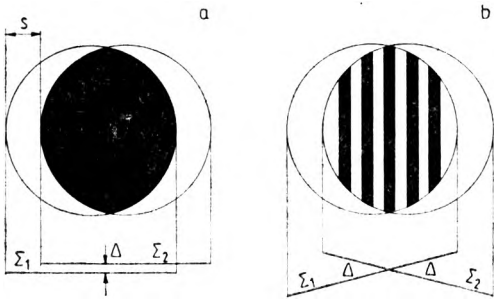


Fig. 2. Exactly focused (a) and slightly defocused (b) shear interference images of an aberration-free microscope objective (the term "focused" means that the objective under testing is focused onto the slit S of the interferometer shown in Fig. 1; consequently, the term "defocused" specifies that the objective is retained in either overfocused or underfocused position with respect to the interferometer slit S)

Normally, the Wollaston prism W is set at a constant distance l_2 behind the objective Ob . This distance directly depends on the mechanical tube length of the objective under examination. Under these conditions, by defocussing the interferometer, i.e., by varying the distance l_3 between the slit S and the objective Ob (Fig. 1), the uniform field interference (Fig. 2a) is changed into fringe interference (Fig. 2b), and vice versa. Simultaneously the distances l_1 and l_5 are varied. When the prism W is slid transversely (p) to the objective axis, the optical path difference Δ (bias retardation) between the split wavefronts Σ_1 and Σ_2 is changed (Fig. 2a), thus the colour (if white light is used) or brightness (if monochromatic light is used) of the uniform field interference is altered or interference fringes (Fig. 2b) are shifted laterally.

The wavefronts Σ_1 and Σ_2 (Fig. 2) represent, in fact, the duplicated Fourier transform of the delta function. The larger the lateral shear s is, the greater the apex angle α of the Wollaston prism W (Fig. 1). When the objective Ob suffers from aberrations, the plane wavefronts Σ_1 and Σ_2 (Fig. 2) are deformed and neither the uniform field interference nor regular fringes will be obtained. Figure 3 shows typical interference patterns when the objective under examination suffers from great negative spherical aberration such as the one occurring for

uncorrected positive lenses. As can be seen, no uniform interference arises for the focused position of objective (Fig. 3b), whereas slightly defocused interference patterns (Figs. 3a and c) contain a number of arched or oval fringes. Nearly the same deformation of the interference patterns occurs when the objective suffers from a great overcorrected (positive) spherical aberration (Fig. 4). In this case, however, the shape of interference fringes is more complicated than in Fig. 3.

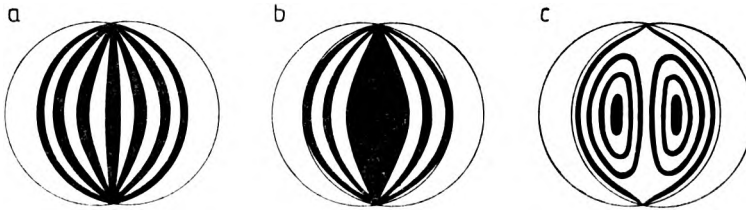


Fig. 3. Underfocused (a), optimally focused (b) and overfocused (c) shear interference images of a microscope objective which suffers from considerable negative spherical aberration

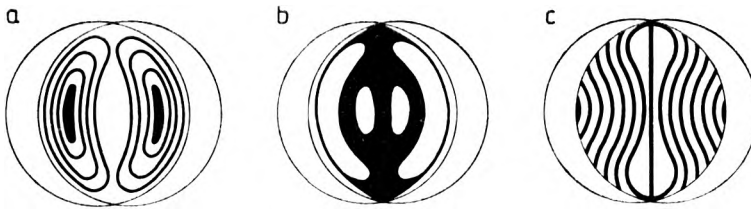


Fig. 4. Underfocused (a), optimally focused (b) and overfocused (c) shear interference images of a microscope objective which suffers from considerable positive spherical aberration

When the microscope objective under examination does not suffer from comatic aberration and/or astigmatism, the interference patterns – such as shown in Figs. 2–4 – retain exactly the same shape when the objective is rotated around its optic axis. Otherwise, one observes a change in configuration of interference fringes. Figure 5 shows typical interference patterns with hyperbolic and elliptic fringes which indicate that the objective under examination suffers from a great axial coma. If the objective is rotated through 360° the patterns shown in Figs. 5a and 5b appear alternately at every 90° . The interferometer

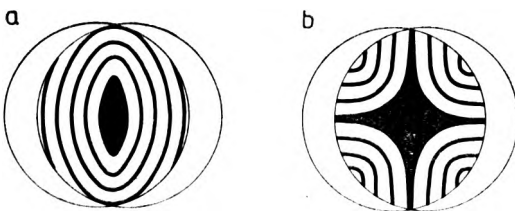


Fig. 5. Shear interference images (optimally focused) of an objective which suffers from considerable axial comatic aberration: a) coma parallel to shear axis, b) coma perpendicular to shear axis. One passes from (a) to (b) by rotating the objective through an angle of 90°

(Fig. 1) is provided with a rotatable socket RS just for the detection of coma and other asymmetric aberration. Coma is frequently coupled with astigmatism. The latter aberration manifests itself by a rotation of the interference fringes when the interferometer is more and more defocused.

The interference patterns, such as shown in Figs. 2–5, refer to extremely poor objectives which are completely inadequate for any microscopical work. From the author's experience it results that modern high-quality microscope objectives give interference patterns such as (or nearly such as) shown in Fig. 2; spherical aberration is not perceived if the wavefront shear s is not larger than 25 % of the exit pupil diameter of the objective.

The interferometer (Fig. 1) comprises four interchangeable birefringent prisms W with different apex angles $\alpha = 5^\circ, 10^\circ, 15^\circ$ and 20° , and four slides with slits of various width w defined by

$$w = \frac{\lambda}{8M_{\text{ob}}(n_e - n_o)\tan\alpha} \quad (1)$$

where λ is the wavelength of used light (for white light $\lambda \approx 0.55 \mu\text{m}$), M_{ob} – the magnification of the objective under examination, and $n_e - n_o$ – the birefringence of a material of which the Wollaston prisms are made (quartz crystal). The slit S must be oriented exactly parallel with respect to the apex edge of the prism W and located at the optic axis of interferometer. For this purpose the stage, on which the slit slide is placed, is rotatable around the said optic axis and translatable transversely to this axis in two perpendicular directions. The interferometer does not need a high-power light source, and a low-voltage lamp (6V/15 W) is quite sufficient for visual observation of interference patterns.

Apart from wave aberrations, this interferometer enables the detection of many other defects, such as optical inhomogeneities in lenses, strain birefringence, errors in shape of lens surfaces etc. Its performance and testing potentialities are illustrated by a great number of interferograms taken with this instrument and presented in the former paper [2] as well as in Ref. [3]. Thus, this documentation will be omitted here.

3. System with variable direction of tilt of laterally sheared wavefronts

One of the basic features of the interferometer described above (Fig. 1) is that the tilt of the wavefronts Σ_1 and Σ_2 (Fig. 2) occurs only around an axis perpendicular to the shear axis. This tilt is accomplished by defocusing the interferometer. Such a tilt in a single direction makes it sometimes very difficult to interpret quantitatively the resulting interference pattern and it was left to many researchers to design wavefront shearing interferometers with the more convenient tilt around the shear axis (for a more detailed discussion of this problem the reader is referred to a review paper by BRIERS [4]).

A few years ago the author noticed that in the interference system such as shown in Fig. 1 [5], instead of the planar slit S a birefringent fibre might be used.

system an additional polarizer P_3 (Fig. 6) must be inserted behind the objective Ob under examination. This polarizer is crossed with P_1 and the fibre B forms an angle of 45° with the directions of light vibrations (P_1P_1 and P_3P_3) of both polarizers. The fibre B is oriented parallel to the wedge edges of the Wollaston prism W whereas the condenser slit CS can be rotated around the optic axis of condenser. If CS is parallel to B , the interferometric system functions similarly to that shown in Fig. 1. If, however, the slit CS forms an angle θ with the fibre axis, the situation is quite different; no uniform field interference ever occurs and always, even with perfectly focused aberration-free objective, there is fringe interference pattern. For a particular value of θ the interference fringes become parallel to the direction of shear of the exit pupil of the objective (Fig. 7c).

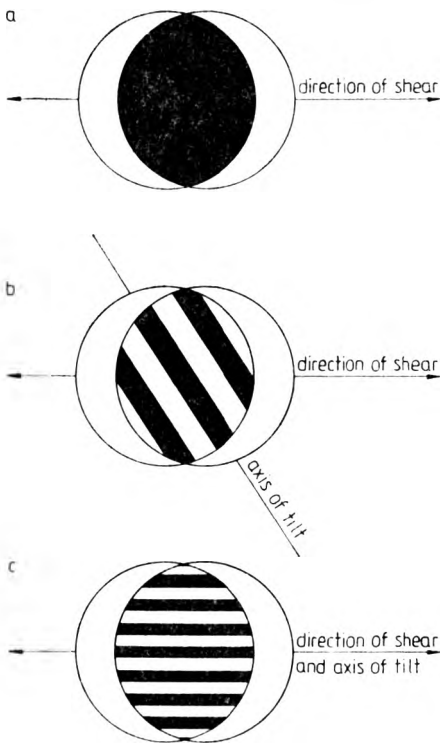


Fig. 7. Exactly focused shear interference images of an aberration-free microscope objective, examined by means of the double-refracting interferometer, optical system of which is shown in Fig. 6. Condenser slit CS is parallel with respect to the birefringent fibre B (a), slit CS is rotated only slightly with respect to the previous position (b), slit CS is oriented to the birefringent fibre B at such an angle θ as to obtain interference fringes parallel with the direction of wavefront shear (c)

Such a configuration of interference fringes shows that the tilt of the sheared wavefronts varies continuously with its amount and direction when the condenser slit CS (Fig. 6) is rotated around the optic axis of condenser.

The use of the tilt of wavefront around the shear axis (Fig. 7c) makes simpler the interpretation of lateral shearing interferograms and improves the sensitivity of the interferometer. These features are illustrated in Figs. 8d and 9c which represent optimally focused interference images of an objective which suffers only from small spherical aberration. The residual aberration is not perceived or hardly visible when the preceding interferometric system (Fig. 1)

is used, but with the new system (Fig. 2) it is easily observed as a bend of interference fringes near the edges of the exit pupil of the objective (Fig. 8d).

If an objective to be examined is corrected for a cover glass, the slit S (Fig. 1) or birefringent fibre B (Figs. 6 and 10) must be covered with a cover slip CG of a proper thickness. Otherwise, spherical aberration will occur.

When the optimally focused objective is rotated around its optic axis (Fig. 11), the use of wavefront tilt around the shear axis causes that coma mani-

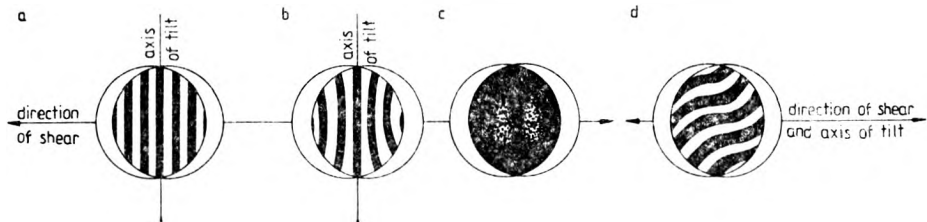


Fig. 8. Shear interference images of a microscope objective which suffers from very small spherical aberration: a) slightly underfocused image, condenser slit CS of the interferometer shown in Fig. 6 is parallel to the birefringent fibre B , b) slightly overfocused image CS is parallel to B , c) optimally focused image, CS is parallel to B , d) optimally focused image, CS is oriented with respect to B at such an angle θ as to obtain interference fringes parallel with the direction of wavefront shear in the central region of the interference pattern

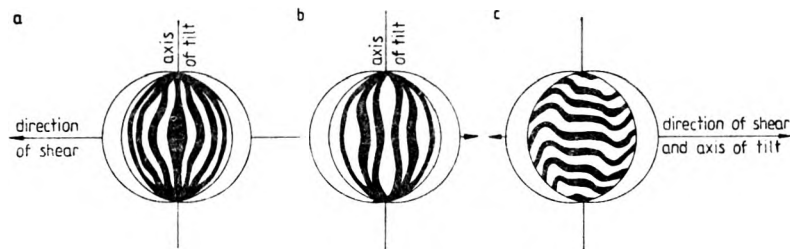


Fig. 9. Interference images of a microscope objective which suffers from significant overcorrected spherical aberration in the marginal zone of the exit pupil: a) slightly underfocused image, condenser slit CS of the interferometer shown in Fig. 6 is parallel to the birefringent fibre B , b) slightly overfocused image, CS is parallel to B , c) optimally focused image, CS is oriented with respect to B at such an angle θ as to obtain interference fringes parallel with the direction of wavefront shear in the central area of the interference pattern

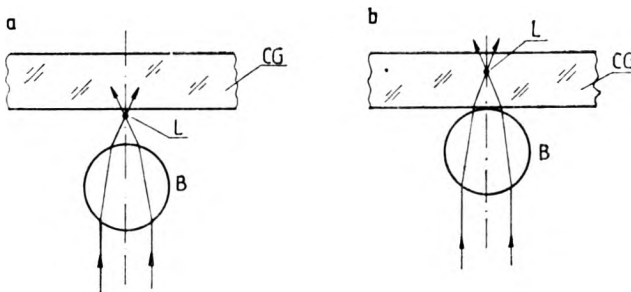


Fig. 10. Correct (a) and incorrect (b) position of the cover glass CG , with respect to the focal line L of the birefringent fibre B

feats itself as more or less arched interference fringes. Astigmatism manifests itself by change in fringe spacing and/or tilt when the objective is rotated through 90° .

4. Selection of the birefringent fibre

When surrounded by the air, a birefringent fibre (oriented diagonally between two crossed polarizers) acts as a high-power bifocal cylindric lens (Fig. 12). Its focal lengths f_{\parallel} and f'_{\perp} , i.e., the distances from the fibre centre to the focal lines L_{\parallel} and L'_{\perp} , are defined by

$$f'_{\parallel} = \frac{r}{2} \frac{n_{\parallel}}{n_{\parallel} - 1} \tag{2a}$$

$$f'_{\perp} = \frac{r}{2} \frac{n_{\perp}}{n_{\perp} - 1} \tag{2b}$$

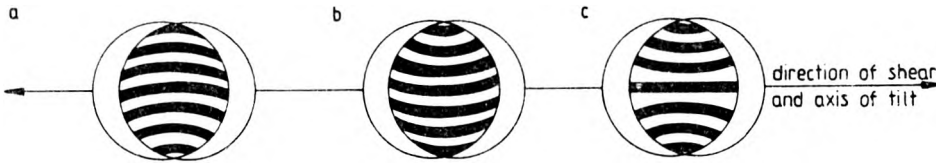


Fig. 11. Optimally focused interference images of a microscope objective which suffers from comatic aberration: a) and b) coma perpendicular to shear axis, c) coma parallel to shear axis. The condenser slit (CS) of the interferometer (Fig. 6) is oriented at such an angle Θ with respect to the birefringent fibre as to obtain interference fringes parallel with the direction of wavefront shear in the central region of the interference patterns. One passes from (a) to (b) by rotating CS through $+\Theta$ and $-\Theta$, and from (a) or (b) to (c) by rotating the objective under test through an angle of 90°

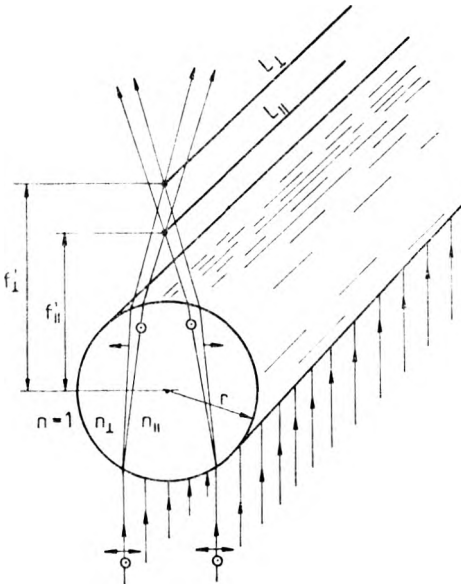


Fig. 12. Birefringent fibre as a bifocal cylindric lens

where $2r$ is the fibre diameter, n_{\parallel} and n_{\perp} are the refractive indices of fibre for light components vibrating parallel and perpendicular to the fibre axis, respectively. The interferometer under discussion needs a birefringent fibre, difference $\Delta f'$ in local lengths ($\Delta f' = f'_{\parallel} - f'_{\perp}$) being very small. It has been stated that $\Delta f'$ must be smaller than $0.2 \mu\text{m}$. In this case the focal lines L_{\parallel} and L_{\perp} act as a single slit or Dirac δ -function, Fourier transform of which is constant over the exit pupil of the objective under testing. Examples of correctly and incorrectly selected fibres are shown in Figs. 13–15. The width w of the focal lines is normally small being additionally diminished by the condenser slit CS (Fig. 6). In any case, w may be smaller than $0.5 \mu\text{m}$. The brightness of the focal lines being also important, is defined approximately by

$$I = I_{\max} \sin^2 \frac{\varphi}{2} \quad (3)$$

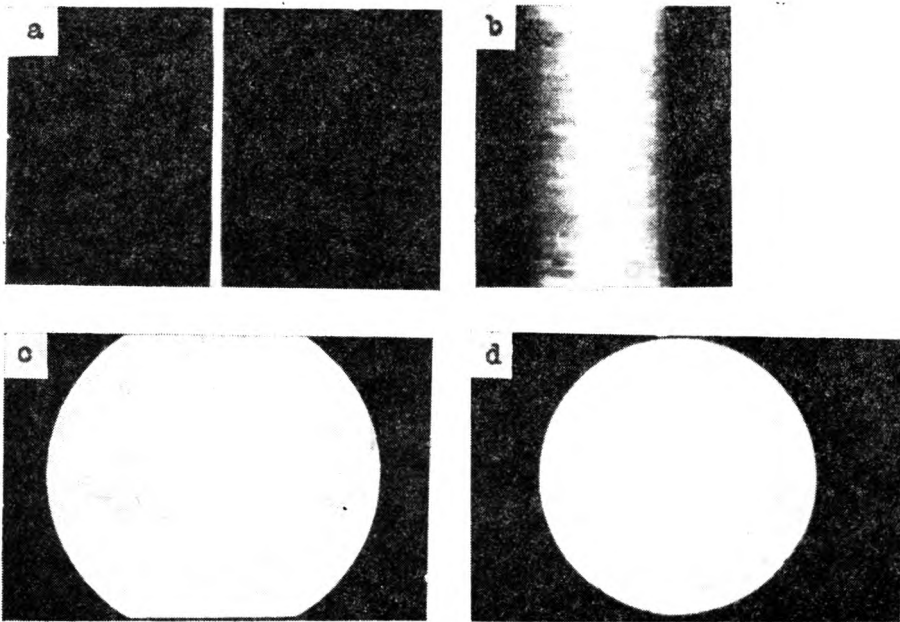


Fig. 13. Birefringent fibre suitable for the interferometer shown in Fig. 6. Focal line of the fibre (a), microscopic image of the fibre (b), optical Fourier transform of the focal line, objective $20 \times / 0.40$ (c), optical Fourier transform of the focal line, objective $40 \times / 0.65$ (d). These transforms are observed when the Wollaston prism is removed from the interferometer shown in Fig. 6. Basic parameters of the fibre are as follows: $2r = 60 \mu\text{m}$, $n_{\parallel} = 1.5515$, $n_{\perp} = 1.5500$, $n_{\parallel} - n_{\perp} = 0.0015$, $f'_{\parallel} = 42.20 \mu\text{m}$, $f'_{\perp} = 42.27 \mu\text{m}$, $\Delta f' = 0.07 \mu\text{m}$

where $\varphi = 2\pi\delta/\lambda$, $\delta = 2r(n_{\parallel} - n_{\perp})$, λ is the wavelength of light (for white light $\lambda = 0.55 \mu\text{m}$), and I is the intensity of light emerging from the focal lines. As can be seen, the maximum brightness of the focal lines is achieved when $\delta = \lambda/2$ or $\delta = (2m - 1)\lambda/2$ (here $m = 1, 2, 3, \dots$).

In the experiments performed, some textile polymer fibres have been successfully used. Their diameters $2r$ ranged from 8 to 60 μm . The interferometer operates both in the white and the monochromatic light.

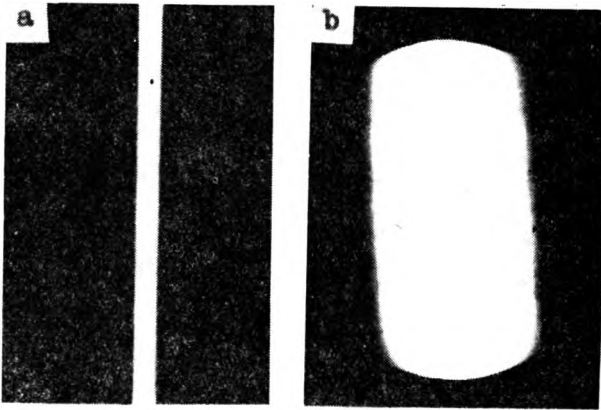


Fig. 14. Birefringent fibre unsuitable for shearing interferometry with variable wavefront tilt. Focal line of the fibre (a), optical Fourier transform of the focal line (b). This focal line acts as a Gaussian function, thus its Fourier transform is also the Gaussian function

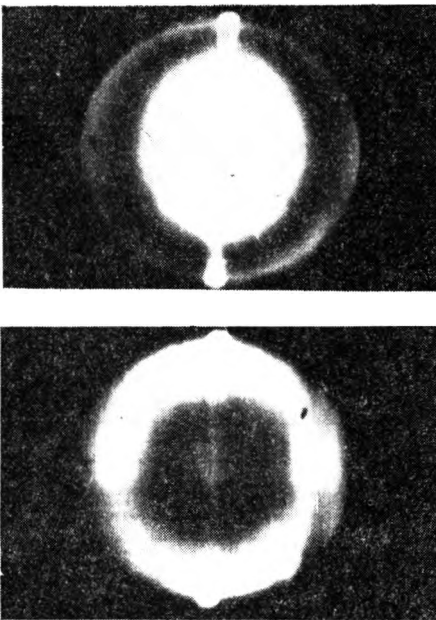


Fig. 15. Optical Fourier transforms of another birefringent fibre unsuitable for shearing interferometry with variable wavefront tilt. Successive photographs were taken in monochromatic light of different wavelength. Basic parameters of the fibre: $2r = 24 \mu\text{m}$, $n_{\parallel} = 1.743$, $n_{\perp} = 1.555$, $n_{\parallel} - n_{\perp} = 0.188$, $f'_{\parallel} = 14.08$, $f'_{\perp} = 16.76 \mu\text{m}$, $\Delta f' = 2.68 \mu\text{m}$. Objective $60\times/0.80$. The fibre acts as two separated slits (focal lines) one of which follows the other along the optic axis of the objective (compare Fig. 12)

5. Discussion and conclusion

The interferometers described above are suitable for the examination of microscope objectives corrected at a finite tube length, whereas infinitely corrected objectives can be tested with these instruments if used with a proper tube lens which focuses the slit S (Fig. 1) or focal lines of a birefringent fibre B (Fig. 6) inside the Wollaston prism W .

A polarization interferometer for testing microscope objectives was also designed by Nomarski. However, Nomarski's instrument operates in reflected light and has a mirror instead of a slit S (Fig. 1) in the object plane of the objective under examination. The light from an epi-illuminator passes twice, back and fourth, through a special birefringent prism (double-refracting "diasporameter") and the objective. This prism is able to produce shearing varying continuously [6], without varying the direction of wavefront tilting.

It is worth noting that a suggestion of using an interference arrangement for testing microscope objectives was first given by Twyman in 1923 [7]. His instrument was derived from the Michelson interferometer. The spatial separation of two interfering waves makes this instrument very sensitive to vibration, thus for every test the two arms of the interference system must be readjusted to equalize their optical paths. These drawbacks make the Twyman interferometer useless for testing microscope objectives today. Next, a series of common-path interferometers have been developed, in which both the test and reference waves follow almost the same path. These instruments are reviewed in papers [4] and [8]. The double-refracting systems presented here (Figs. 1 and 6) belong to this category; they are insensitive to vibrations and other external disturbances.

Recently, an interferometer for testing microscope objectives of high quality has also been developed by researchers from VEB Carl Zeiss Jena [9].

The interpretation of shearing interferograms is not as simple as that of Twyman interferograms, since the interference occurs between two identical wavefronts rather than between one aberrated wavefront (from the objective under test) and one perfect, spherical or plane, wavefront (from a reference mirror). The use of tilt around the shear axis, first introduced by Bates in a version of Mach-Zehnder shearing system [10], greatly reduces this problem for the common-path interferometers. The manipulation with the Bates system is indeed highly complicated, when comparing with the author's system (Fig. 6), the construction and manipulation of which are exceptionally simple.

References

- [1] PLUTA M., *Pomiary, Automatyka, Kontrola* 9 (1963), 292-295 (in Polish).
- [2] PLUTA M., *Optyka* 2 (1967), 5-12, 51-61 (in Polish).
- [3] PLUTA M., *Optical Microscopy* (in Polish), PWN, Warszawa 1984, Chap. 4.
- [4] BRIERS J. D., *Optics and Laser Technol.* 4 (1972), 28-41.
- [5] PLUTA M., *Proc. of the ICO-11*, [in] *Optica Hoy y Mañana*, Eds. J. Bescós et al., Instituto de Optica, Madrid 1978, p. 663-666.
- [6] ROBLIN G., NOMARSKI G., *Nouv. Rev. d'Optique* 2 (1971), 105-113.
- [7] TWYMAN F., *Prism and Lens Making*, Hilger and Watts, London 1952.
- [8] STEEL W. H., *J. Sci. Instrum.* 42 (1965), 102-104.
- [9] FREITAG W., GROSSMANN W., *Jenacr Rundschau* 25 (1980), 168-169.
- [10] BATES W. J., *Proc. Phys. Soc.* 59 (1947), 940-950.

Received October 1, 1981

Интерферометр сдвига с переменным наклоном поперечно смещенных волновых фронтов

Разработан новый интерферометр для тестирования микроскопических объективов. Интерферометр работает в поляризованном свете. Его главными оптическими элементами являются: симметрическая призма Волластона и двоякопреломляющее волокно, использованное как второй источник света. Призма Волластона расщепляет поперечно волновой фронт, в то время как двоякопреломляющее волокно совместно с оборачивающейся щелевой диафрагмой конденсора смещенных волновых фронтов. В выходном зрачке тестируемого объектива наблюдается интерференционная картина.